Environmental Science & Technology

pubs.acs.org/est

Article

Fate and Transformation of 15 Classes of Per- and Polyfluoroalkyl Substances in Aqueous Film-Forming Foam (AFFF)-Amended Soil Microcosms

Sheng Dong,[#] Peng-Fei Yan,[*,#] Katherine E. Manz, Linda M. Abriola, Kurt D. Pennell, and Natalie L. Cápiro[*]

Cite This: https://doi.org/10.1021/acs.est.4c08665

Read Online

ACCESS | Metrics & More | Article Recommendations | Supporting Information

ABSTRACT: The environmental fate of per- and polyfluoroalkyl substances (PFAS) in aqueous film-forming foams (AFFFs), especially those synthesized by electrochemical fluorination (ECF) processes, remains largely unknown. This study evaluated the transformation of AFFF-derived ECF-based precursors in aerobic soil microcosms amended with a historically used AFFF formulation (3M Light Water™). Fifteen classes of PFAS, including AFFF components and transformation products, were identified or tentatively identified by suspect screening/nontargeted analysis (SSA/NTA) throughout a 308-day incubation. This study demonstrates that AFFF-derived ECF-based precursors serve as sources of perfluoroalkane sulfonamides (FASAs) and perfluoroalkyl acids (PFAAs), which are commonly detected at AFFF-impacted sites. Temporal sampling provided evidence for biotransformation of multiple precursors including tri- or dimethyl ammonio propyl perfluoroalkane sulfonamides. Additionally, the environmental stability (i.e., resistance to transformation) of ECF-based precursors was found to depend upon structural characteristics, including perfluoroalkyl chain length, presence of sulfonamide or carboxamide groups, and functional groups (e.g., a branch of carboxyalkyl group) attached to the nitrogen atoms. These findings provide insights into the transformation pathways of AFFF-derived PFAS and other structurally similar ECF-based PFAS, which will support the management and remediation of PFAS contamination at legacy AFFF-impacted sites.

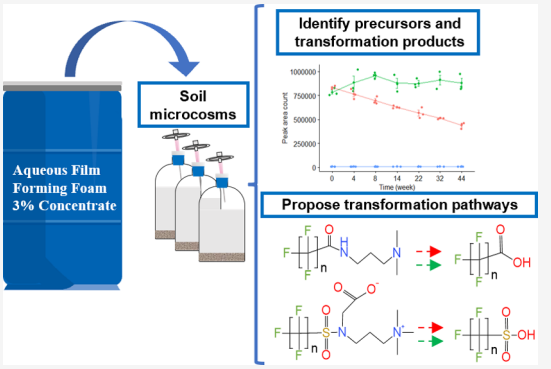

KEYWORDS: *AFFF, per- and polyfluoroalkyl substances (PFAS), sulfonamide- and carboxamide-based precursors, soil microcosm, high resolution mass spectrometry (HRMS), biotransformation*

1. INTRODUCTION

Aqueous film-forming foams (AFFFs) have been effectively used to extinguish hydrocarbon- and solvent-based fires at military, industrial, and municipal sites.[1,2] Although AFFFs are typically proprietary formulations, most consist of solvents and hydrocarbon surfactants, as well as per- and polyfluoroalkyl substances (PFAS).[3] In addition to the commonly studied perfluoroalkyl acids (PFAAs), an increasing number of polyfluoroalkyl substances (i.e., "precursors") have been identified in various AFFFs.[4−7] Upon the release of AFFF into the environment, precursors can be retained in source areas or migrate to adjacent locations,[8−10] and potentially transform to more persistent PFAAs via abiotic or biotic processes.[11−14] Thus, wide variations between the composition of PFAS identified in AFFFs and those detected at AFFF-impacted sites have been reported.[5,6,15] To implement better management and remediation of legacy AFFF-impacted sites, it is crucial to understand the environmental behavior and fate of precursors in AFFFs.

PFAS can be synthesized by electrochemical fluorination (ECF) or fluorotelomerization (FT) chemistry. In AFFF formulations manufactured by 3M, ECF-based PFAS represent substantial components; while FT-based PFAS dominate in formulations from other manufacturers (e.g., Ansul, Chemguard, Angus, National Foam, etc.).[4,16−18] Extensive research has focused on the biotransformation potential of FT-based precursors, including 6:2 fluorotelomer sulfonate (6:2 FTS),[19−23] fluorotelomer thioether amido sulfonates (FTAoS),[11,12,24] 6:2 fluorotelomer sulfonamide alkylamine (6:2 FTAA),[25] and 6:2 fluorotelomer sulfonamide alkylbetaine (6:2 FTAB).[25,26] Mixed bacterial cultures from activated

Received: August 19, 2024
Revised: November 23, 2024
Accepted: November 25, 2024

sludge,[19,24−26] sediment,[20] and soil have been shown to biotransform these compounds to perfluoroalkyl carboxylates (PFCAs).[11,12] Recently, a growing number of studies have focused on the biotransformation of AFFF-derived ECF-based precursors.[13,14,27,28] Although advanced mass spectrometry techniques has facilitated the identification of these chemicals,[4,5,7,16] the complex nature of AFFF-derived ECF-based precursors with different functionalities (e.g., sulfonyl, tertiary amine, quaternary ammonium, etc.)[7,16] and the analytical challenges associated with studying these precursors and potential transformation intermediates[29] has hampered research progress.

To date, only a few of AFFF-derived ECF-based precursors have been investigated for their biotransformation potential, leaving the environmental fate of many others unknown. For example, while the biotransformation of some carboxamide-based precursors with 8 perfluorinated carbons (C_8) and sulfonamide-based precursors with 6 and 8 perfluorinated carbons (C_6 and C_8) have been investigated,[27,30] other analogues with varied perfluoroalkyl carbon chain lengths, which were also identified in AFFFs[7,16] have not been studied. Although precursors of different perfluoroalkyl carbon chain lengths may share similar biotransformation pathways, they likely exhibit chain-length dependent transformation kinetics due to the differences in physical−chemical properties and enzyme specificity.[31] Moreover, previous studies only investigated the transformation kinetics and pathways of standalone precursors (i.e., the target precursor was spiked into the experimental system).[27,30] However, precursor transformation kinetics and extent at AFFF-impacted sites may differ from those in prior studies using standalone precursor[27,30] due to the presence of AFFF-derived nonfluorinated surfactants.

To address the knowledge gaps related to the environmental fate of ECF-based precursors, particularly at AFFF-impacted sites, the current study focuses on a historically used 3M AFFF formulation, which was spiked into microcosms containing soil sourced from a former U.S. military base (i.e., an AFFF-impacted site). The primary objective was to evaluate the environmental fate and transformation of the AFFF-derived ECF-based precursors and elucidate the associated transformation products and pathways. With suspect screening/nontargeted analysis (SSA/NTA) using liquid chromatography-coupled with high resolution mass spectrometry (LC-HRMS), the current study investigates a broad spectrum of AFFF-derived PFAS, including legacy PFAS (e.g., PFCAs and perfluoroalkanesulfonic acids-PFSAs), and a range of novel anionic, zwitterionic, and cationic PFAS classes over a 308-day incubation.[4−7] Based on the temporal changes of these PFAS classes, the associated abiotic and/or biotic transformation pathways in the soil are proposed. Additionally, the transformation extent of multiple ECF-based precursors with similar structures is compared to explore the potential influence of structural characteristics on the environmental fate of ECF-based PFAS.

2. MATERIALS AND METHODS

2.1. Chemicals and Materials. All PFAS analytical standards, including 13 compounds used for targeted analysis and 42 used for suspect screening/nontargeted analysis (NTA/SSA), were purchased from Wellington Laboratories (Guelph, Ontario, Canada) and listed in the Supporting Information (SI), Table S1 and Text S1. The AFFF formulation used in this study is a 1999-era 3M Light Water™ AFFF concentrate (FC-203CF), which was kindly provided by Dr. Paul Hatzinger at APTIM. This formulation has been used by the U.S. military since 1993.[32] Despite being phased out of production after 2002, stocks of legacy AFFF may still be found in fire departments today due to its long shelf life.[33]

The soil used in this study (referred to hereafter as Loring soil) was collected from a location proximate to a fire station at the former Loring Air Force Base (Aroostook County, ME), which had been contaminated by historical AFFF application. Previous microcosm studies demonstrated that the native microbial community in Loring soil is capable of biotransforming fluorotelomer precursors.[34−36] Properties and PFAS contamination of Loring soil have been previously documented.[34,35] Prior to use, the soil was homogenized, ground, sieved (ASTM E11 #10 size), and stored at 4 °C.

2.2. Microcosm Setup and Sampling Procedure. Microcosms were prepared in 60 mL Wheaton serum bottles, each containing 30 mL of mineral growth medium and 3 g (dry weight) of Loring soil. The medium was prepared according to the recipe reported by Löffler et al.[37] excluding resazurin, L-cysteine, and sodium sulfide. Additionally, diethylene glycol butyl ether (DGBE), was added, as it is an organic solvent present in the AFFF formulation and can serve as an electron donor and carbon source for microbial growth.[11,35] Three treatments were prepared: (1) a live treatment, in which 30 μL of AFFF concentrate (0.1% v/v) was spiked; (2) an abiotic control, in which 30 μL of AFFF concentrate was spiked along with the addition of 1 g/L sodium azide to inhibit microbial activity; and (3) a live control, in which only 1.2 mM DGBE was spiked (the equivalent amount of DGBE added in the live treatment and abiotic control through the addition of AFFF containing 20% (v/v) DGBE). Each bottle was sealed with a rubber septum and an aluminum cap. In order to maintain aerobic conditions, air was introduced to the microcosms by penetrating the septa with a syringe needle connected to a 0.22 μm sterile polyethersulfone (PES) syringe filter (VWR, Radnor, PA). All microcosms were incubated at room temperature on a horizontal platform shaker (Innova 2350, New Brunswick Scientific) at 150 rotations per minute (rpm) for a period of 308 days.

At each sampling time (day 0, 28, 56, 98, 154, 224, and 308), three bottles from the live treatment and two bottles from the abiotic and live controls were destructively sampled following an established procedure.[34] Briefly, 0.5 mL of supernatant from each bottle was first collected and mixed with 9.5 mL methanol for the analysis of PFAS in the microcosm aqueous phase. One milliliter of well-mixed slurry was then collected for the analysis of dissolved organic carbon (DOC) (TOC-L CPH, Shimadzu), a proxy of DGBE consumption. The remaining solid phase was collected by centrifuging the remaining slurry (4000 rpm, 20 min) and discarding the supernatant. The collected solid was vortexed in 30 mL methanol for 30 min followed by sonication in a water bath at 60 °C for 30 min. Following centrifugation at 4000 rpm for 20 min, an aliquot of methanol extract was transferred to a 15 mL centrifuge tube and diluted with 9 mL methanol for PFAS analysis. Both aqueous and soil extract samples were filtered through 0.45 μm Whatman GMF syringe filter (Cytiva, Marlborough, MA) and stored at −20 °C prior to targeted and nontargeted PFAS analysis. It should be noted that the extraction process for microcosm solids and the filtration of PFAS samples with syringe filters prior to analysis have been applied in previous studies without reported issues of PFAS

https://doi.org/10.1021/acs.est.4c08665
Environ. Sci. Technol. XXXX, XXX, XXX−XXX

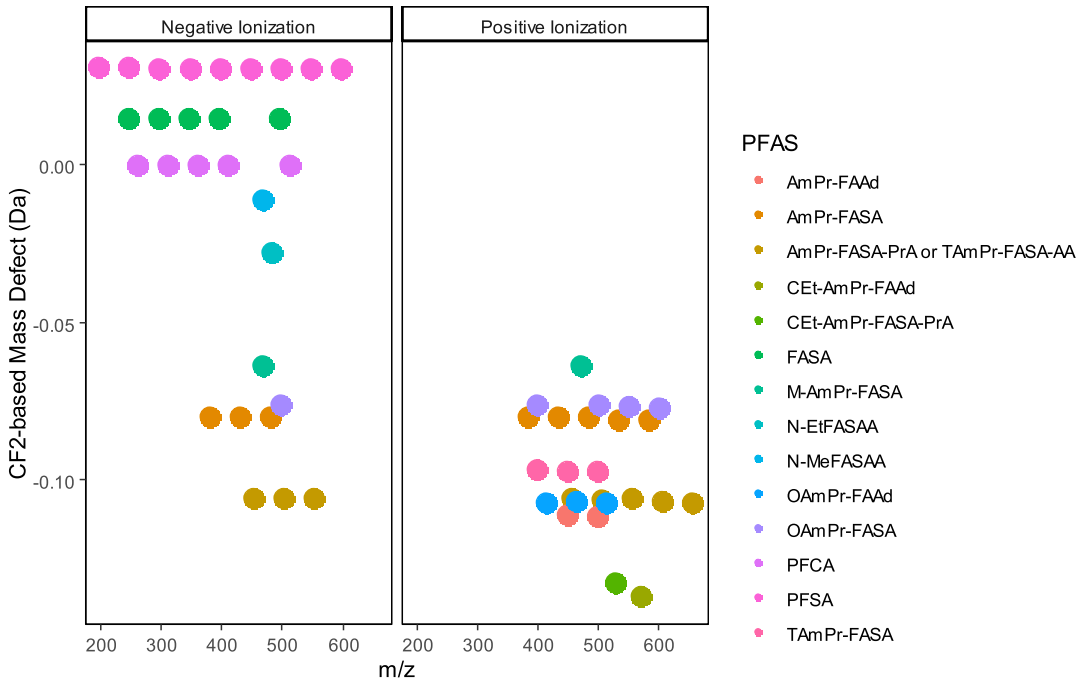

Figure 1. Kendrick Mass Defect (KMD) plot for CF_2 repeating units vs mass-to-charge ratio for the series of PFAS detected in SSA/NTA analysis.

mass loss.[22,34,38−40] However, such practices may result in partial mass loss and/or omission of certain PFAS compounds in the current study, given the complex PFAS composition in the AFFF microcosms (i.e., 15 PFAS classes identified as described in Section 3.1). Future studies are suggested to consider alternative methods for solid extraction and pretreatment for aqueous microcosm samples if necessary. For example, repeated extraction with methanol solution containing a chemical base and cleanup using solid-phase extraction (SPE) cartridges before analysis is considered to minimize potential false-negative results.

2.3. Suspect Screening/Nontargeted Analysis (SSA/NTA). *2.3.1. Instrument and Data Acquisition.* SSA/NTA analysis was conducted on a Thermo QExactive HF-X Orbitrap MS equipped with a Vanquish ultrahigh-performance liquid chromatograph (UHPLC-Orbitrap). The MS with electrospray ionization was operated in both positive (ESI+) and negative (ESI−) ionization modes. Detailed instrumental settings and procedures for SSA/NTA analysis are described in Table S2 and SI-Text S1. Note that the NTA Study Reporting Tool (SRT) was used in the preparation of this manuscript (10.6084/m9.figshare.19763503 [Excel]).[41] The LC-HRMS data were analyzed by Thermo Compound Discoverer (CD) 3.3 software following the processing workflow as described previously[34] and in Text S1. Spectral libraries and mass lists were used to identify AFFF-derived PFAS compounds and associated transformation products. The libraries included Thermo mzCloud and an in-house MS^2 mass spectral library containing 42 PFAS compounds. The mass lists included 88 hypothesized AFFF-derived PFAS compounds and associated transformation products based on previous studies (Table S3), and 8142 fluorinated compounds from the EPA's CompTox Chemicals Dashboard.[42] Two final feature tables containing a total of 4492 and 9521 features were obtained from ESI+ and ESI− modes, respectively.

To select the features of interest, the two feature tables were first screened based on the following criteria: (a) the coefficient of variation (CV) was <30% in replicate injections for more than 1 sample; (b) the area counts were >500,000 in positive ionization mode (ESI+) or >100,000 in negative ionization mode (ESI−) for at least one sampling point; (c) at least one of the Compound Discoverer reported Mass Defects for CF_2, C_2F_4, and CF_3 was below 0.8; and (d) an accurate mass error <5 ppm.

2.3.2. Categorization of AFFF Components and Transformation Products. The selected features in SSA/NTA analysis were further screened and classified as follows: (1) an AFFF Component: if peak area counts of a feature at day 0 in the live treatments and abiotic controls were significantly larger ($p < 0.05$) than those in the live controls, the compound was selected and regarded as an AFFF component; and (2) an AFFF Transformation Product: if peak areas of a feature at day 0 in the live treatments and abiotic controls were below the threshold (i.e., 500,000 area counts in ESI+ and 100,000 area counts in ESI− mode), but increased significantly afterward and above the threshold, the compound was selected and regarded as a transformation product of AFFF components. Confidence levels were assigned to each selected compound based on established criteria.[43] In addition, the selected compounds with a different number of repeating CF_2 units (where one CF_2 moiety has an exact mass of 49.9968 m/z) were regarded as homologues within one PFAS class.

2.3.3. Comparison of the Environmental Stability of AFFF Components. To facilitate comparisons of the environmental stability (i.e., transformation or formation extent) of AFFF components during the 308-day microcosm experiments, $\log_2$-fold changes (LFCs) in the associated peak area counts between day 308 and day 0 were calculated using LFC = log2 (peak area count on day 308/peak area count on day 0). A negative LFC represents a decrease in the total mass of one PFAS (i.e., transformation occurred); the lower (more negative) the LFC was, the greater transformation occurred and vice versa. Considering the comparison consistency and

https://doi.org/10.1021/acs.est.4c08665
Environ. Sci. Technol. XXXX, XXX, XXX−XXX

overall data availability, the data from ESI+ mode were used to calculate all LFCs of identified AFFF components.

2.4. Targeted PFAS Analysis. To verify the PFAS temporal changes as characterized in peak area counts from SSA/NTA analysis, targeted analysis was conducted for 13 PFAS compounds using commercially available analytical standards (as listed in Table S1). Concentrations of these PFAS in microcosm aqueous sample and soil extracts were determined on an Vanquish Flex Binary UPLC system (Thermo Scientific) coupled to a quadrupole orbitrap mass spectrometer (Orbitrap Exploris 120, Thermo Scientific). The method for quantification of these targeted PFAS is shown in SI-Text S2. The instrument limits of detection (LODs) and limits of quantification (LOQs) are listed in Table S4.

3. RESULTS AND DISCUSSION

3.1. PFAS Identified and Tentatively Identified by SSA/NTA Analysis in AFFF-Amended Microcosms. A total of 15 classes of PFAS were identified or tentatively identified (confidence level 1−4) throughout the 308-day microcosm experiment using the SSA/NTA analysis (Figure 1). The confidence levels are assigned based on established criteria ranging from level 1 (the most likely), confirmed by reference standards, to level 4 (the least likely), determined by an unequivocal molecular formula.[43] Notably, homologues in four classes achieved level 1, while three class attained level 4 and all remaining classes and homologues reached levels 2−3, as detailed in Table S6, along with other information on the PFAS identification used in SSA/NTA analysis (e.g., mass error, retention time). Figure 1 displays the CF_2-based Kendrick Mass Defect (KMD) for these 15 classes based on the KMD analysis of PFAS,[44] where all homologues sharing the same core structure but varying in the number of the CF_2 units exhibit identical KMD values. The full name and corresponding acronym of each PFAS class are provided in Table 1. The acronyms for homologues in each class are listed in Table S5 along with NIST IDs from the NIST Suspect List of PFAS (version 1.8) and their prior occurrences in the literature. The acronyms were adopted from recent publications,[45,46] and an explanation of the naming conventions is provided by Choi et al.[47]

Figure 2 illustrates the chemical structures of the 15 PFAS classes, the homologues identified within each class, and the trends in peak area, representing the change in mass of each PFAS over the microcosm incubation. Among the 15 PFAS classes, 9 were categorized as AFFF components, and 8 were categorized as transformation products (Figure 2). Two classes, PFCAs and PFSAs, were categorized as both AFFF components and transformation products (Figure 2). MS^2 spectra for one representative compound from each class, if available, have been provided in the SI (see Figures S2−S11). In addition, the temporal changes in peak areas for homologues with varying numbers of perfluorinated carbons (C_n, where n denotes the number of perfluorinated carbons in the compound) within each PFAS class during the 308-day incubation are plotted in Figures S12−S25.

Analytical standards were commercially available for 13 individual PFAS compounds within 4 classes, including C_6 AmPr-FASA, C_6 and C_8 FASA, C_3−C_7 PFCA, and C_4−C_8 PFSA. Quantification of these PFAS in the microcosm samples was performed, and the changes in total mass over the 308-day period are shown in Figures S26 and S27. The observed changes in peak area counts of PFAS tentatively identified in the SSA/NTA analysis (Figures S13, S18−S20) corresponded to the temporal changes quantified in the targeted PFAS analysis (Figures S26 and S27), indicating a strong correlation between the two analytical methods.[48]

Table 1. Full Names and Corresponding Acronyms of Classified PFAS Identified and Tentatively Identified in SSA/NTA Analysis

full name	acronym
N-Trimethyl ammonio propyl perfluoroalkane sulfonamide	TAmPr-FASA[a,b,c]
N-Dimethyl ammonio propyl perfluoroalkane sulfonamide	AmPr-FASA[a,b,c]
N-Carboxy ethyl dimethyl ammonio propyl perfluoroalkane sulfonamido propanoic acid	CEt-AmPr-FASA-PrA[a]
N-Dimethyl ammonio propyl perfluoralkane sulfonamido propanoic acid or *N*-trimethyl ammonio propyl perfluoroalkane sulfonamide acetic acid	AmPr-FASA-PrA[a,b] or TAmPr-FASA-AA
N-Carboxy ethyl dimethyl ammonio propyl perfluoroalkane amide	CEt-AmPr-FAAd
N-Dimethylammonio propyl perfluoroalkane amide	AmPr-FAAd[a,b,c]
Perfluoroalkanesulfonic acids	PFSA[a,b]
Perfluoroalkyl carboxylic acid	PFCA[a,b]
Perfluoroalkane sulfonamide	FASA[a,b,c]
N-Methyl ammonio propyl perfluoroalkane sulfonamide	M-AmPr-FASA[c]
N-Oxide dimethyl ammonio propyl perfluoroalkane sulfonamide	OAmPr-FASA[a,b]
N-Methyl perfluoroalkane sulfonamido acetic acid	N-MeFASAA[a,b]
N-Ethyl perfluoroalkane sulfonamido acetic acid	N-EtFASAA[b]
N-Oxide dimethyl ammonio propyl perfluoroalkane amide	OAmPr-FAAd

[a]PFAS in this class have been documented in historical AFFF formulation(s).[4,5,7,16,17] [b]PFAS in this class have been found in environmental matrices, including AFFF-impacted soil and groundwater.[5−7,9,10,45,46] [c]C_8 homologue in in this class have been reported to undergo biotransformation or appear as transformation products from PFAA precursors.[13,14,27]

3.1.1. AFFF Components. 3.1.1.1. TAmPr-FASA. This PFAS class is characteristic of a perfluoroalkyl sulfonamide base structure with propyl trimethylammonium (Figure 2). C_4−C_6 TAmPr-FASA homologues were detected in ESI+ mode with confidence level 2 (Table S5). Recent studies reported the occurrence of this PFAS class in both historical AFFFs[7,17] and AFFF-impacted soils and groundwater.[9,10,45,46] In the present study, peak areas of C_4−C_6 TAmPr-FASA homologues gradually decreased by >99.5, 60.1, and 31.0% on average in live treatments during the 308-day incubation (Figure S12). In contrast, the mass of these homologues remained relatively constant in abiotic controls. These results suggest that TAmPr-FASA could be biotransformed by the native microbes in Loring soil but were stable under abiotic conditions. The observed susceptibility of TAmPr-FASA to biotransformation corroborates a previous study that reported the biotransformation of C_8 homologue of TAmPr-FASA in soil.[13]

3.1.1.2. AmPr-FASA. This class (C_4−C_8 homologues identified or tentatively identified in both ESI+ and ESI− modes with confidence levels 1−3) shares the same base structure as TAmPr-FASA, except one methyl group in trimethylammonium is replaced by a hydrogen atom (Figure 2). While multiple homologues in the AmPr-FASA class were previously identified in several AFFF formulations,[16,17] multiple studies have only been able to detect them sporadically in AFFF-impacted soil and groundwater samples.[5,9,10,45,46] The infrequent detection of AmPr-FASA in AFFF-impacted sites

https://doi.org/10.1021/acs.est.4c08665
Environ. Sci. Technol. XXXX, XXX, XXX−XXX

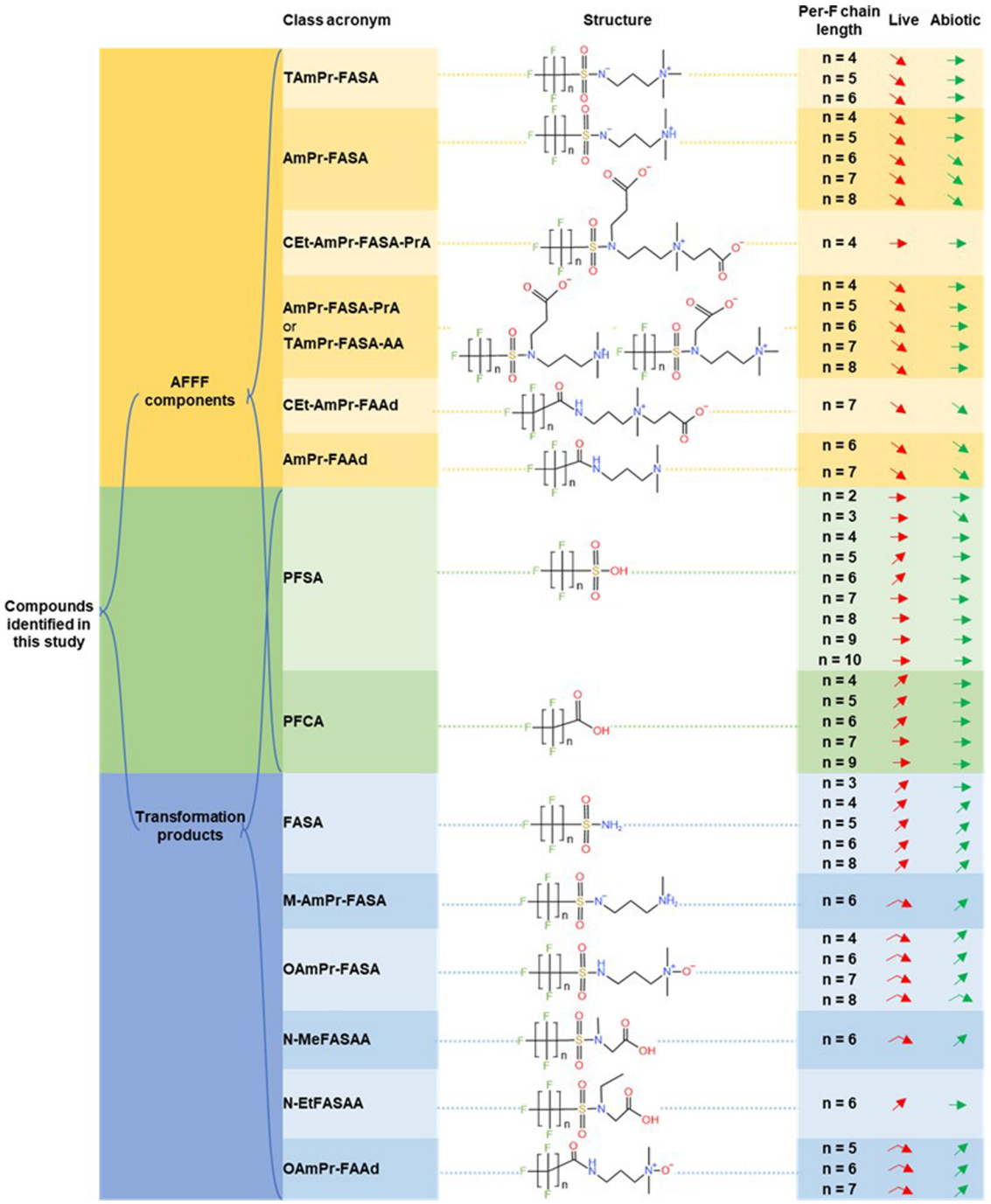

Figure 2. Fifteen classes of PFAS tentatively identified and/or identified by SSA/NTA analysis in AFFF-amended microcosms, including 9 classes categorized as AFFF components (shaded in yellow), 8 classes categorized as transformation products (shaded in blue), and 2 classes as both AFFF components and transformation products (shaded in green). Chemical structures of the PFAS classes are illustrated. General trends of peak area in live treatment and abiotic control over the 308-day incubation of each homologue within each class were depicted with arrows: upward arrows for increase, downward arrows for decrease, horizontal arrows for no significant change, and bent arrows for trends with both upward and downward movements within the experimental period.

was attributed to their susceptibility to transformation.[6] In this study, biotransformation of C_4−C_8 AmPr-FASA homologues was observed in the live treatment, where the peak areas of C_4−C_8 homologues decreased by 47.4−93.6% after 308 days (Figure S13). Possible abiotic transformation was also observed in abiotic controls, but only for the long-chain C_6−C_8 homologues and with a slower rate (10.6−53.7% decrease in peak areas) (Figure S13).

3.1.1.3. CEt-AmPr-FASA-PrA. This class (C_4 homologue tentatively identified with confidence 3 in ESI+ mode) comprises the base structure of *TAmPr-FASA* and two additional propionate groups on the tertiary sulfonamide nitrogen and the quaternary ammonium terminal (Figure 2). Homologues in this PFAS class were previously detected in various AFFF formulations,[4,16,17,49] yet their environmental stability has not been investigated. In the present study, no obvious decrease in peak areas of the C_4 homologue of CEt-

https://doi.org/10.1021/acs.est.4c08665
Environ. Sci. Technol. XXXX, XXX, XXX−XXX

AmPr-FASA-PrA class was observed during the 308-day incubation (Figure S14), suggesting its persistence under abiotic and biotic conditions within the time scale of this study.

3.1.1.4. AmPr-FASA-PrA or TAmPr-FASA-AA. AmPr-FASA-PrA features a propionate group linked to the sulfonamide nitrogen in AmPr-FASA, while TAmPr-FASA-AA contains an acetate branch on the sulfonamide nitrogen in TAmPr-FASA (Figure 2). SSA/NTA analysis suggested the presence of either or both isomeric classes with C_4−C_8 homologues (confidence level 3). Previous studies reported the occurrence of AmPr-FASA-PrA homologues in AFFF formulations,[4,5,16,17] and AFFF-impacted sites.[5,10,45,46] Conversely, the TAmPr-FASA-AA class has not been reported in AFFF formulations or the environment. Furthermore, the environmental stability of either class has not been previously reported. In this study, the peak areas of C_4−C_8 homologues within AmPr-FASA-PrA or TAmPr-FASA-AA class decreased by 43.3−84.6% in the live treatments after 308-day incubation (Figure S15). In contrast, such decreases were not observed in the abiotic controls (Figure S15). These results suggest that either or both PFAS classes were readily susceptible to biotic transformation but remained abiotically stable under the experimental conditions.

3.1.1.5. AmPr-FAAd. This PFAS class (C_6−C_7 homologues tentatively identified in ESI+ mode with confidence level 3) is an analogue to AmPr-FASA, with the sulfonamide group replaced by a carboxamide group (Figure 2). Previously, the AmPr-FAAd class was detected in AFFF formulations and a commercial surfactant,[16] as well as AFFF-impacted soils.[10] In the present study, rapid abiotic transformation of AmPr-FAAd was observed in microcosms, with the peak areas of C_6 and C_7 homologues decreasing by 81.9−82.3% in the abiotic control after the 308-day incubation (Figure S16). Biotransformation of AmPr-FAAd was also observed, as greater decreases (90.2−91.3%) in the peak areas of C_6 and C_7 homologues were detected in the live treatment (Figure S16). These findings are consistent with results of previous studies where the C_8 homologue of AmPr-FAAd was shown to be transformed through abiotic and biotic processes.[13,14,27] These results suggest that the AmPr-FAAd class is unlikely to be persistent in the environment and can be readily transformed after an AFFF release.

3.1.1.6. CEt-AmPr-FAAd. This class (C_7 homologue tentatively identified in ESI+ mode with confidence level 4) has the same base structure as AmPr-FAAd with an additional carboxylethyl branch on the tertiary amine to make it a quaternary ammonium (Figure 2). Neither the occurrence in AFFF formulations nor the biotransformation potential of CEt-AmPr-FAAd has been reported previously. In this study, gradual and similar decreases (45.2 ± 7.6%) in the peak areas of CEt-AmPr-FAAd were observed in both the live treatment and abiotic control during the 308-day incubation (Figure S17). This finding suggests that CEt-AmPr-FAAd could be transformed abiotically in the microcosms, but the extent of biotransformation may be minimal.

3.1.1.7. PFCA and PFSA. These two commonly investigated PFAS classes were also identified (confidence level 1−2) in the present AFFF formulation, with C_4−C_7 and C_9 PFCAs and C_2−C_{10} PFSAs detected in ESI- mode (Figure 2). The detection of PFCAs and PFSAs was in agreement with previous studies that reported PFCAs (e.g., 0−170 mg/L for C_4−C_9 PFCAs) and PFSAs (e.g., 6,700−15,000 mg/L for PFOS) as minor and major PFAS components, respectively, of ECF-based AFFF formulations.[5] The environmental persistence of PFCAs and PFSAs has been widely acknowledged,[6,50] which contributes to their presence in AFFF-impacted soils and groundwater.[4,5,8−10] In this study, no decrease in the peak areas of any homologue within PFCAs and PFSAs was observed (Figures S18 and S19), indicating their high stability in the microcosms. In addition, certain homologues (e.g., PFHxS, the C_6 PFSA) demonstrated increased peak areas (Figure S18), likely due to their formation during the transformation of aforementioned precursors and those discussed in Section 3.1.2.

3.1.2. Transformation Products. 3.1.2.1. FASA. C_3−C_6 and C_8 homologues (detected in ESI- mode with confidence levels 1−2) were formed during the transformation of precursors in the AFFF formulation, especially under biotic conditions. As shown in Figure S20, peak areas of FASAs increased notably (factors 5.8−410.8) in live treatments over 308 days, while abiotic controls showed a smaller increase (factors of 1.4−5.0). These findings could explain the widespread detection of FASAs in AFFF-impacted soil and groundwater samples, despite the fact that FASAs were rarely present in AFFF formulations.[6,7,9,10,17,45] Further biotransformation of FASAs to PFSAs (e.g., C_8 homologue, FOSA to PFOS) was previously documented, with a wide range in the biotransformation rate (half-lives of 9.2−712 days).[51−54] In the present study, biotransformation of FASAs likely occurred, as suggested by a slower increase in the peak areas of FASAs between days 98 and 154 (Figure S20). However, the overall formation rate exceeded the transformation rate of FASAs, resulting in a substantial accumulation of FASAs over the 308-day incubation period.

3.1.2.2. M-AmPr-FASA. This PFAS class (C_6 homologue tentatively identified in ESI+ and ESI− modes with confidence level 3 or 4) shares the same base structure as AmPr-FASA with one methyl terminus substituted by a hydrogen atom (Figure 2). The peak areas of C_6 M-AmPr-FASA increased substantially in the first 98 days of incubation (by a factor of 82.1 and 34.5 in ESI+ and ESI− modes, respectively), and subsequently decreased in the live treatments (Figure S21). Conversely, in the abiotic controls, the peak areas continued to increase over 308 days (by factors of 10.3−18.2), indicating that abiotic formation of M-AmPr-FASA was much slower than biotic formation. The presence of M-AmPr-FASA was likely to result from the transformation of TAmPr-FASA and AmPr-FASA; the two classes that were previously reported to be precursors of M-AmPr-FASA,[13,14,27] and were also detected in the present study (see Section 3.1.1). Further biotransformation of M-AmPr-FASA was also reported previously,[13,14,27] consistent with the decreasing trends observed in the live treatments after day 98 in this study (Figure S21). In addition, only C_6 homologue of M-AmPr-FASA was detected in the microcosms despite the detections of C_4−C_6 TAmPr-FASA and C_4−C_8 AmPr-FASA (see Section 3.1.1). The absence of other M-AmPr-FASA homologues was likely due to their rapid conversion to downstream products.[13,14,27]

3.1.2.3. OAmPr-FASA. This class (C_4 and C_6−C_8 homologues tentatively identified in ESI+ and ESI− modes with confidence level 3) shares the same base structure as TAmPr-FASA with trimethylammonium replaced by a dimethylamine oxide (Figure 2). OAmPr-FASA was previously reported in AFFF formulations,[16,17] and AFFF-impacted groundwater and soil.[7,10,45] In the present study, OAmPr-FASA was determined as intermediate transformation products rather than AFFF components (Figure S22). The peak areas of C_4 and C_6

https://doi.org/10.1021/acs.est.4c08665
Environ. Sci. Technol. XXXX, XXX, XXX−XXX

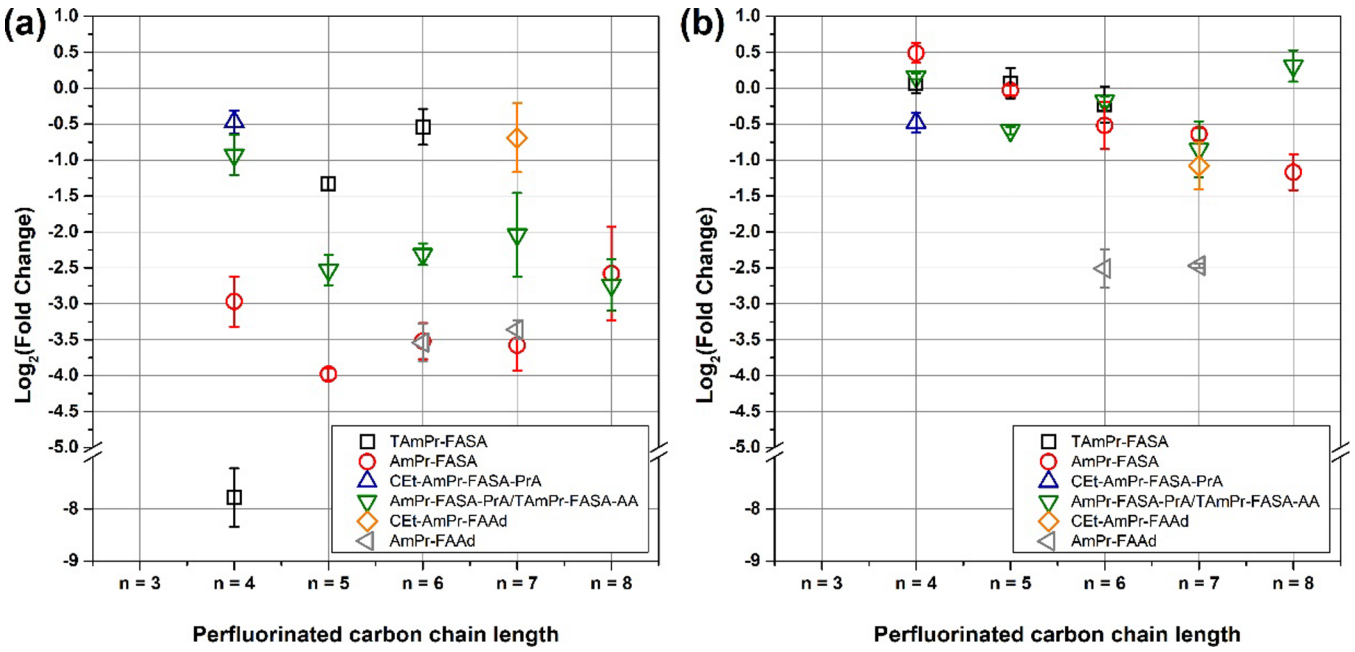

Figure 3. Log_2-fold changes (LFCs) in peak areas of PFAS classes tentatively identified and/or identified by SSA/NTA analysis as AFFF components between day 308 and day 0 in (a) live treatment and (b) abiotic control, respectively. Error bars represent one standard error among replicate microcosms.

homologues in the live treatments continuously increased from day 0 to day 98 (by factors of 7.1−34.0), then sharply decreased until day 154 (Figure S22); afterward, the peak areas increased again from day 154 until day 224 (by a factor of 9.8−13.5), followed by a second decrease (Figure S22). Similar trends of peak area were observed for C_7 and C_8 homologues in the live treatments, but with 1 to 2 orders-of-magnitude lower peak area counts (Figure S22). In addition, the formation of C_4 and C_6−C_8 homologues was observed in the abiotic controls (by factors of 5.5−60.6), and a decrease of the C_8 homologue was observed after day 154 (Figure S22). These results indicate that OAmPr-FASA was readily formed from AFFF components (see Section 3.1.1) through biotic and abiotic transformation processes. Moreover, the biotic transformation of OAmPr-FASA was more rapid than abiotic transformation under the experimental conditions.

3.1.2.4. N-MeFASAA and N-EtFASAA. These two classes (C_6 homologues tentatively identified with confidence level 4 in ESI− mode) share a perfluoroalkane sulfonamido acetate chain. N-MeFASAA has a methyl group on the sulfonamide nitrogen, while N-EtFASAA has an ethyl group (Figure 2). Although N-EtFASAA was not previously found in AFFF formulations, N-MeFASAA was detected in an AFFF formulation[17] and the occurrence of both classes was reported in AFFF-impacted soil and groundwater samples.[7,9,10,45] In the present study, the peak areas of C_6 N-MeFASAA increased greatly by a factor of 15.3 in the first 98 days, then decreased by half at the end of the incubation in the live treatments (Figure S23), suggesting its initial formation from AFFF components followed by biotransformation. In the abiotic controls, the peak area of C_6 N-MeFASAA gradually increased by a factor of 2.6 during the incubation (Figure S23), indicating that C_6 N-MeFASAA can also be formed by abiotic processes at a slower rate. For C_6 N-EtFASAA, a rapid and substantial increase in the peak areas (171.8 times increase) was observed in the live treatments, while no distinguishable change was found in the abiotic controls over 308-day incubation (Figure S24). This finding suggests that the formation of N-EtFASAA was primarily due to biotransformation of its precursor(s).

3.1.2.5. OAmPr-FAAd. This class (C_5−C_7 homologues tentatively identified with confidence level 3 in ESI+ mode) is a structural analogue to OAmPr-FASA, but the sulfonamide functional group is substituted by a carboxamide group (Figure 2). In the live treatment, the peak areas of C_5−C_7 homologues increased by factors of 13.0−29.5 at day 98 compared to day 0, and decreased to nearly 0 at day 154, then increased again (Figure S25). In contrast, a continuous increase in OAmPr-FAAd was observed in the abiotic controls; at the end of incubation, the peak area increased by factors of 28.8−48.2 (Figure S25). These results indicate that OAmPr-FAAd readily formed under both biotic and abiotic conditions; however, transformation of OAmPr-FAAd rapidly occurred under biotic conditions, while it was slow or infeasible under abiotic conditions. The rapid biotransformation of OAmPr-FAAd observed here is consistent with a prior study that reported 50% biotransformation of C_8 OAmPr-FAAd within 3−7 days in soil microcosms.[14] Also, these findings are consistent with the rare detection of OAmPr-FAAd in AFFF-impacted environments.

3.1.2.6. PFCA and PFSA. Under biotic conditions, increases in PFSAs (C_3−C_6 homologues, by factors of 1.6−2.7) and PFCAs (C_4−C_6 homologues, by factors of 1.5−1.6) were observed in microcosms (Figures S18 and S19) due to the biotransformation of AFFF components and intermediate products (discussed in Sections 3.1.1 and 3.1.2). Under abiotic conditions, only C_4 and C_{6-7} PFSAs were found to form at a slower rate (peak areas increased by factors of 1.2−1.5) (Figure S18), indicating the possibility of a higher abundance of C_4 and C_{6-7} homologue PFSA-precursors and associated abiotic transformation potential. The formation of PFCAs and PFSAs is consistent with previous studies which documented

https://doi.org/10.1021/acs.est.4c08665
Environ. Sci. Technol. XXXX, XXX, XXX−XXX

the two PFAS classes as stable transformation products of FT- and ECF-based precursors.[13,14,27]

3.2. Structurally Relevant Factors Impacting the Stability of AFFF Components. The transformation extent of AFFF-derived PFAS, especially the AFFF precursor components, varied widely. These differences in stability likely resulted from the structural variations among these PFAS compounds. In this section, three structurally relevant factors (carbon chain length of perfluorinated moiety, presence of functional group linking the perfluorinated moiety with the nonfluorinated moiety, and the presence of a secondary nitrogen) were identified as impacting the stability of AFFF-derived ECF-based precursors by comparing the behavior of those sharing similar structures.

First, the carbon chain length of perfluorinated moiety within ECF-based precursors was found to likely influence the stability, especially under biotic conditions (Figure 3). LFCs of homologues in TAmPr-FASA, AmPr-FASA, and AmPr-FASA-PrA/TAmPr-FASA-AA in the live treatments increased with the elongation of perfluorinated carbon chain (Figure 3a), suggesting a longer perfluorinated carbon chain could render higher microbial stability. Specifically, LFCs for C_4, C_5, and C_6 homologues of TAmPr-FASA in the live treatment were -7.78 ± 0.56, -1.33 ± 0.09, and -0.54 ± 0.25, respectively (Figure 3a). LFCs for C_5−C_8 homologues of AmPr-FASA increased from -3.98 ± 0.08 to -2.58 ± 0.65, and C_5−C_7 homologues of AmPr-FASAA-PrA/TAmPr-FASA-AA increased from -2.53 ± 0.21 to -2.04 ± 0.58 (Figure 3a). Unexpectedly, LFCs for C_4 homologues of AmPr-FASA and AmPr-FASAA-PrA/TAmPr-FASA-AA were greater than corresponding C_5 homologues (Figure 3a). This observation could be due to more rapid formation of C_4 homologues from their precursors than formation of C_5 homologues, resulting in a smaller overall decrease in C_4 homologues. In contrast to biotic conditions, the influence of perfluorinated carbon chain length on the abiotic transformation of these ECF-based precursors was not observed (Figure 3b). These findings suggest that the influence of perfluorinated carbon chain length on PFAS biotransformation is likely attributed to increased hydrophobicity as the perfluorinated carbon chain elongates. Higher hydrophobicity could increase the binding affinity of PFAS to soil particles within the microcosms, reducing their bioavailability to microorganisms.

Second, some classes (e.g., AmPr-FASA) of ECF-based precursors harbor a sulfonamide group ($-SO_2-N(H)-$) while others (e.g., AmPr-FAAd) contain a carboxamide group ($-C(O)-N(H)-$), both of which link the perfluorinated moiety with nonfluorinated moiety (Figure 2). Results from this study suggest that the presence of these two functional groups impact PFAS stability under biotic and abiotic conditions. Compared to AmPr-FASA, much more rapid transformation of AmPr-FAAd was observed in abiotic controls (Figures S13 and S16), as indicated by lower LFCs for C_6 and C_7 AmPr-FAAd (-2.51 ± 0.27 and -2.47 ± 0.03) than the AmPr-FASA analogues (-0.52 ± 0.33 and -0.64 ± 0.08) (Figure 3a). This suggests that carboxamide-based PFAS were less stable compared to sulfonamide-based analogues under abiotic conditions, likely due to the lower resistance of carboxamides to abiotic hydrolysis.[55] The abiotic transformation of another carboxamide-based PFAS class, CEt-AmPr-FAAd, also demonstrated the abiotic transformation susceptibility of carboxamides (Figure S7). Under biotic conditions, rapid transformation of both AmPr-FASA and AmPr-FAAd was observed in live treatment (Figures S13 and S16), as indicated by close LFCs (ca. −3.5) for both PFAS classes (Figure 3a). Rapid transformation was also observed for OAmPr-FASA and OAmPr-FAAd following initial production of these compound classes (e.g., from day 98 to 154 in live treatment) as shown in Figures S22 and S25. These observations contradict previous studies that reported sulfonamide-based PFAS were more microbially stable than their carboxamide counterparts.[27] This discrepancy could be due to the fact that the sulfonamide- and carboxamide-based PFAS classes compared in this study were both readily biotransformed, masking the slight enhancement of microbial stability by the sulfonamide group.

Third, most ECF-based precursors identified in the present study (e.g., AmPr-FASA and TAmPr-FASA) contain a second nitrogen atom (another amine group) in addition to the first nitrogen in the sulfonamide/carboxamide group (Figure 2). The structural differences on the second nitrogen atom could influence PFAS stability. With three methyl groups on the second nitrogen atom (quaternary ammonium), the PFAS microbial stability appeared to be higher than that with two methyl groups (tertiary amine). For example, LFCs of C_5 and C_6 TAmPr-FASA homologues (-1.33 ± 0.09 and -0.54 ± 0.25) were greater than those of their AmPr-FASA counterparts (-3.98 ± 0.08 and -3.52 ± 0.25) in the live treatment (Figure 3a). The microbial stability of PFAS with one or no methyl groups on the second nitrogen atom (secondary or primary amine) was hypothesized to be even lower. M-AmPr-FASA (with a secondary amine, Figure 2) was detected in this study as an intermediate, and its rapid transformation following initial formation was observed in the live treatment (Figure S21). In addition, an oxygen atom on the tertiary amine headgroup, e.g., OAmPr-FASA and OAmPr-FAAd (Figure 2), rendered low microbial stability, as evidenced by their rapid biotransformation following production (Figures S22 and S25). In contrast, adding a carboxyalkyl group on the tertiary amine headgroup could potentially enhance the resistance of PFAS to both biotic and abiotic transformation. For example, CEt-AmPr-FAAd exhibited higher stability than AmPr-FAAd in the live treatment and abiotic controls (Figure 3); LFCs of C_7 homologue of CEt-AmPr-FAAd were -0.69 ± 0.48 and -1.08 ± 0.33 in the live treatment and abiotic controls, respectively, which were much greater than that for C_7 AmPr-FAAd (-3.36 ± 0.13 and -2.47 ± 0.03, respectively). The findings related to the influence of structural differences in the second amine group on PFAS stability are consistent with a previous study that showed PFAS containing quaternary ammonium or a carboxyalkyl group on tertiary amine groups were more stable than those with a tertiary amine or an oxygen atom on tertiary amine groups.[27]

In addition to the second nitrogen atom, it was found that the presence of a carboxyalkyl group on the first nitrogen atom (i.e., sulfonamide/carboxamide group) further enhanced PFAS stability. For example, CEt-AmPr-FASA-PrA, which contains a carboxyalkyl group on both nitrogen atoms (Figure 2), exhibited a high persistence in the microcosms in the absence of observed abiotic or biotic transformation during the 308-day incubation (Figure S14). Comparatively, if only one carboxyalkyl group is attached on either of the nitrogen atoms, e.g., AmPr-FASA-PrA/TAmPr-FASA-AA and CEt-AmPr-FAAd (Figure 2), the PFAS compounds were susceptible to transformation, which suggests transformation starts at the nitrogen atom without a carboxyalkyl group

https://doi.org/10.1021/acs.est.4c08665
Environ. Sci. Technol. XXXX, XXX, XXX−XXX

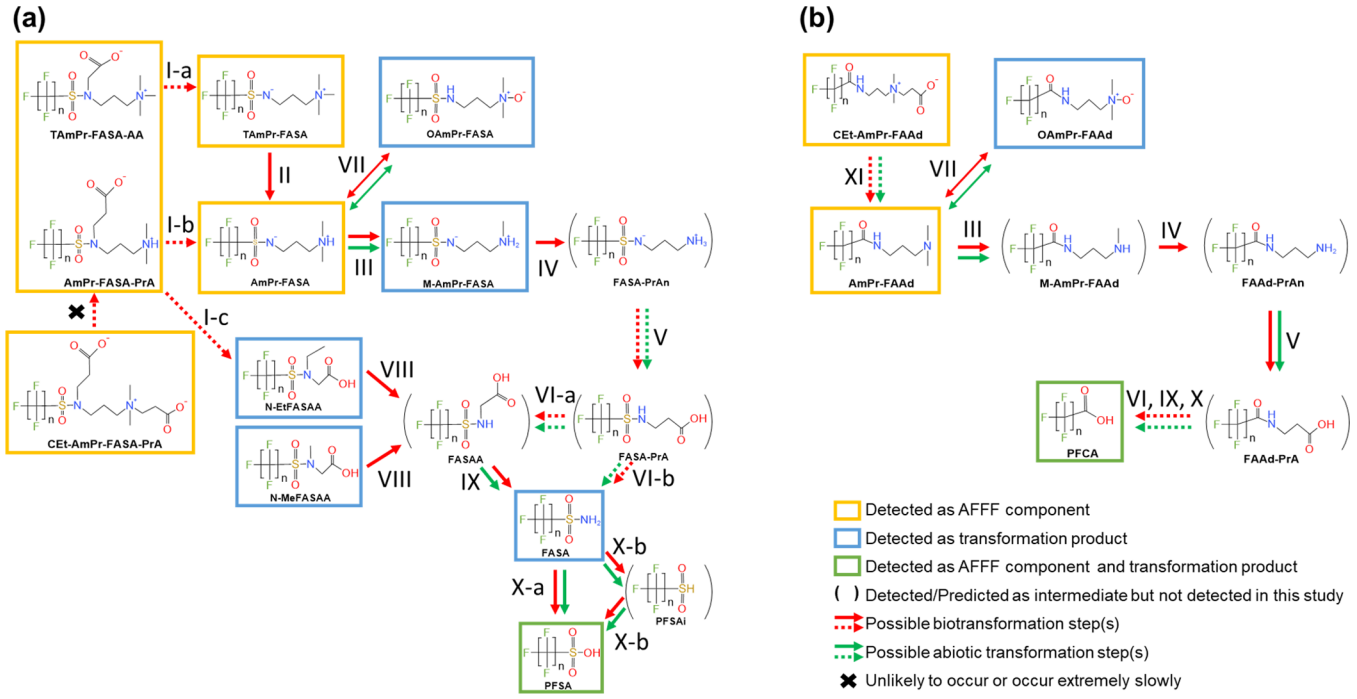

Figure 4. Proposed transformation pathways of (a) sulfonamide-based and (b) carboxamide-based PFAS identified by SSA/NTA analysis in AFFF-amended soil microcosms. Compounds in yellow and blue boxes were categorized as AFFF components and transformation products, respectively. Compounds in green boxes were categorized as both AFFF components and transformation products. Compounds in parentheses were not detected in this study but were detected or predicted as intermediates in previous studies.[13,14,27] Red and green arrows represent possible biotransformation and abiotic transformation steps, respectively. Dashed arrows indicate hypothetical steps.

attached (Figures 2, S15, and S17). Previous studies have documented increased stability when a carboxyalkyl group is present with the sulfonamide group. For example, N-ethyl perfluorooctane sulfonamide (EtFOSA) was readily transformed in soil (half-lives of 11.2−26.8 days), while N-ethyl perfluorooctane sulfonamido acetic acid (EtFOSAA), which has an additional carboxymethyl group on the sulfonamide group, was more resistant to biotransformation (half-lives of 287−653 days).[53,54] Additionally, after the ethyl branch on the sulfonamide group of EtFOSA was oxidized to carboxymethyl, perfluorooctane sulfonamido acetic acid (FOSAA) became more microbially stable (half-lives of 96.2−334 days).[53,54] These current findings and those of previous studies suggest that the presence of a carboxyalkyl group on the nitrogen atom(s) in ECF-based precursors likely hinders N-decarboxylation and N-dealkylation (when an alkyl group is present on the same nitrogen), leading to increased stability.

3.3. Transformation Pathways of Identified AFFF-Derived PFAS. Based on the AFFF components and transformation products identified or tentatively identified by SSA/NTA analysis and their environmental stability as discussed in Sections 3.1 and 3.2, transformation pathways involving 15 AFFF-derived PFAS classes in aerobic soil are proposed in Figure 4.

The abiotic and biotic transformation potentials of CEt-AmPr-FASA-PrA, TAmPr-FASA-AA or AmPr-FASA-PrA were, for the first time, investigated in the current study. With a carboxyalkyl group on each nitrogen atom, CEt-AmPr-FASA-PrA was stable in the soil microcosms (Figure S14); its transformation was less likely or occurred at an extremely slow rate (Figure 4a). As for TAmPr-FASA-AA/AmPr-FASA-PrA, these compounds remained stable under abiotic conditions, while their biotransformation may have proceeded via two different pathways. Pathway I-a/I-b involves decarboxylation and N-dealkylation of the carboxyalkyl branch on the first nitrogen atom, converting TAmPr-FASA-AA or AmPr-FASA-PrA to TAmPr-FASA or AmPr-FASA, respectively (Figure 4a). Pathway I-c involves multiple N-dealkylations of the tertiary/secondary amine head groups on the second nitrogen atom, followed by a deamination reaction, converting TAmPr-FASA-AA or AmPr-FASA-PrA to N-MeFASAA and N-EtFASAA (Figure 4a). The transformation of TAmPr-FASA-AA or AmPr-FASA-PrA may primarily proceed through pathway I-c, given the absence of a carboxyalkyl group on the second nitrogen atom but presence on the first nitrogen.

As an AFFF component and a potential minor product of TAmPr-FASA-AA, TAmPr-FASA was persistent under abiotic conditions, but was susceptible to microbial transformation (Figure S12). One of the methyl groups on the quaternary ammonium headgroup of TAmPr-FASA could be replaced by a hydrogen, leading to the formation of a tertiary amine (i.e., AmPr-FASA) via pathway II (Figure 4a). AmPr-FASA undergoes further transformation through pathways III and IV to lose two methyl groups from the tertiary amines successively through N-dealkylation, forming products with secondary amines (M-AmPr-FASA) and primary amines (FASA-PrAn), respectively (Figure 4a). Through deamination and oxidation in pathway V, FASA-PrAn was then transformed to FASA-PrA, which could be converted to either FASAA via decarboxylation and oxidation (pathway VI-a), or to FASA via further decarboxylation and N-dealkylation (pathway VI-b). Similar transformation from TAmPr-FASA to FASA involving pathways II through VI were proposed previously with C_8 homologues of each PFAS class.[13,27] Substantial formation of OAmPr-FASA was observed in this study under both abiotic and biotic conditions (Figure S22), possibly from the oxidation

https://doi.org/10.1021/acs.est.4c08665
Environ. Sci. Technol. XXXX, XXX, XXX−XXX

of AmPr-FASA through pathway VII (Figure 4a), as proposed recently.[30] The amine oxide in OAmPr-FASA can also be reduced back to tertiary amine as reported previously,[14] resulting in reversible reactions between OAmPr-FASA and AmPr-FASA.

The formation of N-MeFASAA and N-EtFASAA during the transformation of AFFF-derived PFAS was demonstrated for the first time in the current study. As mentioned above, N-MeFASAA and N-EtFASAA might be biotransformation products of TAmPr-FASA-AA/AmPr-FASA-PrA via pathway I-c (Figure 4a). N-MeFASAA and N-EtFASAA were then converted to FASAA through N-dealkylation or a decarboxylation followed by multiple steps of alkyl oxidation (pathway VIII) (Figure 4a).[51,53,56] FASAA could be further transformed to FASA via decarboxylation and N-dealkylation (pathway IX) (Figure 4a).[51,53,54] FASA peak areas increased in both the live treatment and abiotic control (Figure S20), suggesting that FASA can be formed under both biotic and abiotic conditions. FASA was subsequently transformed to PFSA (Figure 4a). The transformation of FASA to PFSA might be a direct process via pathway X-a as reported previously,[14,56] or the transformation may occur through pathway X-b to generate an intermediate PFSAi, as reported in several studies.[27,30,51]

Transformation pathways of carboxamide-based PFAS in the AFFF formulation are illustrated in Figure 4b. The reactions leading AmPr-FAAd to PFCA were similar to its sulfonamide counterpart (Figure 4a). First, successive N-dealkylation occurred to the methyl groups on the second nitrogen of AmPr-FAAd, resulting in the production of M-AmPr-FAAd and FAAd-PrAn through pathways III and IV (Figure 4b). Then, N-deamination followed by oxidation processes converted FAAd-PrAn to FAAd-PrA via pathway V (Figure 4b). FAAd-PrA was further transformed to PFCA through decarboxylation, multiple steps of alkyl oxidation, and amide hydrolysis (pathways VI, IX, and X) (Figure 4b). Similar reactions involving carboxamide-based PFAS (i.e., from AmPr-FAAd to PFCA) were also predicted in previous studies.[14,27,56] The occurrence of CEt-AmPr-FAAd in the AFFF formulation and associated transformation potential were reported in the current study for the first time. It is hypothesized that CEt-AmPr-FAAd could be biotically and abiotically transformed to AmPr-FAAd through decarboxylation and N-dealkylation (pathway XI) (Figure 4b). Similar to AmPr-FASA and OAmPr-FASA, the reactions between AmPr-FAAd and OAmPr-FAAd may be reversible and could occur biotically and abiotically (pathway VI) (Figure 4b).

4. ENVIRONMENTAL IMPLICATIONS

This study identified or tentatively identified 15 classes of PFAS in a historically used 3M AFFF formulation and demonstrated that multiple classes of ECF-based precursors (e.g., C_4−C_8 AmPr-FASA) are susceptible to abiotic and/or biotic transformation across a wide range of homologues, serving as sources of PFAAs at AFFF-impacted sites. For the first time, the biotransformation of AmPr-FASA-PrA/TAmPr-FASA-AA and CEt-AmPr-FAAd has been demonstrated, while CEt-AmPr-FASA-PrA was found to be persistent under the experimental conditions tested. Considering the time frame of this study and the extent of transformation observed, AFFF release into soils will likely lead to long-term PFAS contamination in the source zone and adjacent areas. The widespread detection of similar ECF-based precursors in environmental samples from legacy AFFF-impacted sites suggests that the transformation rates in the field might be slower than those under laboratory conditions. Furthermore, the use of AFFF as the source of parent PFAS compounds provided a broader perspective on the environmental stability of different classes of precursors and different homologues in individual classes. It was found that the functional groups of the nonfluorinated moiety and the carbon chain length of the perfluorinated moiety influenced the stability of these precursors. Notably, the presence of an additional methyl group at the end of the nonfluorinated moiety and carboxyalkyl group(s) on one or both two nitrogen atoms, and a longer perfluorinated carbon chain enhanced the stability of the precursors. This structure-transformation relationship may provide important information to manufacturers regarding the production of biodegradable alternatives to traditional PFAS.

Although the PFAS identified or tentatively identified by SSA/NTA analysis in this study can be assigned with a confidence level based on established criteria (e.g., a match to library MS/MS and retention times, fragmentation evidence, and specific ranges of mass defects), the majority of the PFAS could not be directly quantified due to the lack of authentic standards. Consequently, the availability of these authentic standards will be needed for definitive determinations of environmental occurrence, and detailed investigations of PFAS environmental fate. Moreover, due to the complex composition and transformation pathways of the AFFF-derived PFAS, the transformation kinetics of individual precursors could not be determined in the current study. Further studies are needed to gain a deeper understanding of transformation mechanisms and rates of AFFF precursors. With increased knowledge of precursor stability and transformation, environmental professionals and regulators can make informed decisions about potential contamination risks and develop more effective remediation strategies.

■ ASSOCIATED CONTENT

Supporting Information

The Supporting Information is available free of charge at https://pubs.acs.org/doi/10.1021/acs.est.4c08665.

Details regarding chemicals, targeted LC−MS and SSA/NTA LC−HRMS analyses, full names and acronyms of classified PFAS, profiles of PFAS identified and tentatively identified by SSA/NTA analysis (peak area) and PFAS quantified by targeted LC−MS analysis (mass), mass lists of hypothesized AFFF-derived PFAS compounds and associated transformation products based on previous studies, Compound Discoverer workflow and parameters, and MS^2 spectra of representative PFAS identified or tentatively identified (PDF)

■ AUTHOR INFORMATION

Corresponding Authors

Peng-Fei Yan − *Department of Biological and Environmental Engineering, Cornell University, Ithaca, New York 14853, United States;* orcid.org/0000-0003-3685-1088; Phone: +1 334 444-7753; Email: py222@cornell.edu

Natalie L. Cápiro − *Department of Biological and Environmental Engineering, Cornell University, Ithaca, New York 14853, United States;* orcid.org/0000-0002-8125-

https://doi.org/10.1021/acs.est.4c08665
Environ. Sci. Technol. XXXX, XXX, XXX−XXX

1658; Phone: +1 607 254-2303; Email: natalie.capiro@cornell.edu

Authors

Sheng Dong − *Department of Biological and Environmental Engineering, Cornell University, Ithaca, New York 14853, United States;* orcid.org/0000-0002-6807-4300

Katherine E. Manz − *School of Public Health, University of Michigan, Ann Arbor, Michigan 48109, United States;* orcid.org/0000-0002-8225-9168

Linda M. Abriola − *School of Engineering, Brown University, Providence, Rhode Island 02912, United States;* orcid.org/0000-0003-2420-6145

Kurt D. Pennell − *School of Engineering, Brown University, Providence, Rhode Island 02912, United States;* orcid.org/0000-0002-5788-6397

Complete contact information is available at: https://pubs.acs.org/10.1021/acs.est.4c08665

Author Contributions

#S.D. and P.-F.Y. contributed equally to this work.

Notes

The authors declare no competing financial interest.

■ ACKNOWLEDGMENTS

This work was funded by the Strategic Environmental Research and Development Program (SERDP) under contract W912HQ-18-C-0014 for Project ER18-1149, "Development and Laboratory Validation of Mathematical Modeling Tools for Prediction of PFAS Transformation, Transport, and Retention in AFFF Source Areas" and W912HQ-24-C-0021 for Project ER23-3628, "Environmental Conditions Influencing Natural Abiotic and Biotic Transformation of Perfluoroalkyl Acid (PFAA) Precursors at AFFF-impacted Sites." Acquisition of the Thermo LC Q Exactive HF-X Orbitrap MS was supported by an NSF MRI award (GR5260439). We thank Naji Akladiss at Maine Department of Environmental Protection (MEDE) for providing access to collect Loring soil. We would also like to thank Dr. Paul Hatzinger at APTIM for providing AFFF used in this study and Dr. Melissa Boersma at the Mass Spectrometry Center of Auburn University for her assistance in targeted PFAS analysis.

■ REFERENCES

(1) Moody, C. A.; Field, J. A. Determination of Perfluorocarboxylates in Groundwater Impacted by Fire-Fighting Activity. *Environ. Sci. Technol.* **1999**, *33* (16), 2800−2806.

(2) Tuve, R. L.; Jablonski, E. J. Method of Extinguishing Liquid Hydrocarbon Fires. US3258423A, June 28, 1966. https://patents.google.com/patent/US3258423A/en (accessed 2021−03−03).

(3) Moody, C. A.; Field, J. A. Perfluorinated Surfactants and the Environmental Implications of Their Use in Fire-Fighting Foams. *Environ. Sci. Technol.* **2000**, *34* (18), 3864−3870.

(4) Place, B. J.; Field, J. A. Identification of Novel Fluorochemicals in Aqueous Film-Forming Foams Used by the US Military. *Environ. Sci. Technol.* **2012**, *46* (13), 7120−7127.

(5) Backe, W. J.; Day, T. C.; Field, J. A. Zwitterionic, Cationic, and Anionic Fluorinated Chemicals in Aqueous Film Forming Foam Formulations and Groundwater from U.S. Military Bases by Nonaqueous Large-Volume Injection HPLC-MS/MS. *Environ. Sci. Technol.* **2013**, *47* (10), 5226−5234.

(6) Houtz, E. F.; Higgins, C. P.; Field, J. A.; Sedlak, D. L. Persistence of Perfluoroalkyl Acid Precursors in AFFF-Impacted Groundwater and Soil. *Environ. Sci. Technol.* **2013**, *47* (15), 8187−8195.

(7) Barzen-Hanson, K. A.; Roberts, S. C.; Choyke, S.; Oetjen, K.; McAlees, A.; Riddell, N.; McCrindle, R.; Ferguson, P. L.; Higgins, C. P.; Field, J. A. Discovery of 40 Classes of Per- and Polyfluoroalkyl Substances in Historical Aqueous Film-Forming Foams (AFFFs) and AFFF-Impacted Groundwater. *Environ. Sci. Technol.* **2017**, *51* (4), 2047−2057.

(8) Adamson, D. T.; Nickerson, A.; Kulkarni, P. R.; Higgins, C. P.; Popovic, J.; Field, J.; Rodowa, A.; Newell, C.; DeBlanc, P.; Kornuc, J. J. Mass-Based, Field-Scale Demonstration of PFAS Retention within AFFF-Associated Source Areas. *Environ. Sci. Technol.* **2020**, *54* (24), 15768−15777.

(9) Adamson, D. T.; Kulkarni, P. R.; Nickerson, A.; Higgins, C. P.; Field, J.; Schwichtenberg, T.; Newell, C.; Kornuc, J. J. Characterization of Relevant Site-Specific PFAS Fate and Transport Processes at Multiple AFFF Sites. *Environmental Advances* **2022**, *7*, No. 100167.

(10) Nickerson, A.; Rodowa, A. E.; Adamson, D. T.; Field, J. A.; Kulkarni, P. R.; Kornuc, J. J.; Higgins, C. P. Spatial Trends of Anionic, Zwitterionic, and Cationic PFASs at an AFFF-Impacted Site. *Environ. Sci. Technol.* **2021**, *55* (1), 313−323.

(11) Harding-Marjanovic, K. C.; Houtz, E. F.; Yi, S.; Field, J. A.; Sedlak, D. L.; Alvarez-Cohen, L. Aerobic Biotransformation of Fluorotelomer Thioether Amido Sulfonate (Lodyne) in AFFF-Amended Microcosms. *Environ. Sci. Technol.* **2015**, *49* (13), 7666−7674.

(12) Yi, S.; Harding-Marjanovic, K. C.; Houtz, E. F.; Gao, Y.; Lawrence, J. E.; Nichiporuk, R. V.; Iavarone, A. T.; Zhuang, W.-Q.; Hansen, M.; Field, J. A.; Sedlak, D. L.; Alvarez-Cohen, L. Biotransformation of AFFF Component 6:2 Fluorotelomer Thioether Amido Sulfonate Generates 6:2 Fluorotelomer Thioether Carboxylate under Sulfate-Reducing Conditions. *Environ. Sci. Technol. Lett.* **2018**, *5* (5), 283−288.

(13) Mejia-Avendaño, S.; Vo Duy, S.; Sauvé, S.; Liu, J. Generation of Perfluoroalkyl Acids from Aerobic Biotransformation of Quaternary Ammonium Polyfluoroalkyl Surfactants. *Environ. Sci. Technol.* **2016**, *50* (18), 9923−9932.

(14) Chen, H.; Liu, M.; Munoz, G.; Duy, S. V.; Sauvé, S.; Yao, Y.; Sun, H.; Liu, J. Fast Generation of Perfluoroalkyl Acids from Polyfluoroalkyl Amine Oxides in Aerobic Soils. *Environ. Sci. Technol. Lett.* **2020**, *7* (10), 714−720.

(15) Yan, P.-F.; Dong, S.; Pennell, K. D.; Cápiro, N. L. A Review of the Occurrence and Microbial Transformation of Per- and Polyfluoroalkyl Substances (PFAS) in Aqueous Film-Forming Foam (AFFF)-Impacted Environments. *Science of The Total Environment* **2024**, *927*, No. 171883.

(16) D'Agostino, L. A.; Mabury, S. A. Identification of Novel Fluorinated Surfactants in Aqueous Film Forming Foams and Commercial Surfactant Concentrates. *Environ. Sci. Technol.* **2014**, *48* (1), 121−129.

(17) Hao, S.; Choi, Y.-J.; Wu, B.; Higgins, C. P.; Deeb, R.; Strathmann, T. J. Hydrothermal Alkaline Treatment for Destruction of Per- and Polyfluoroalkyl Substances in Aqueous Film-Forming Foam. *Environ. Sci. Technol.* **2021**, *55* (5), 3283−3295.

(18) Cao, D.; Schwichtenberg, T.; Duan, C.; Xue, L.; Muensterman, D.; Field, J. Practical Semiquantification Strategy for Estimating Suspect Per- and Polyfluoroalkyl Substance (PFAS) Concentrations. *J. Am. Soc. Mass Spectrom.* **2023**, *34* (5), 939−947.

(19) Wang, N.; Liu, J.; Buck, R. C.; Korzeniowski, S. H.; Wolstenholme, B. W.; Folsom, P. W.; Sulecki, L. M. 6:2 Fluorotelomer Sulfonate Aerobic Biotransformation in Activated Sludge of Waste Water Treatment Plants. *Chemosphere* **2011**, *82* (6), 853−858.

(20) Zhang, S.; Lu, X.; Wang, N.; Buck, R. C. Biotransformation Potential of 6:2 Fluorotelomer Sulfonate (6:2 FTSA) in Aerobic and Anaerobic Sediment. *Chemosphere* **2016**, *154*, 224−230.

(21) Yan, Pengfei Biotransformation of Perfluorooctane Sulfonamide (FOSA), 8:2 Fluorotelomer Alcohol (8:2 FTOH), and 6:2 Fluorotelomer Sulfonate (6:2 FTS) in Aqueous Film-Forming Foam (AFFF)-Impacted Soils under Oxic and Anoxic Conditions. Auburn University, 2022.

(22) Yan, P.-F.; Dong, S.; Manz, K. E.; Woodcock, M. J.; Liu, C.; Mezzari, M. P.; Abriola, L. M.; Pennell, K. D.; Cápiro, N. L. Aerobic Biotransformation of 6:2 Fluorotelomer Sulfonate in Soils from Two Aqueous Film-Forming Foam (AFFF)-Impacted Sites. *Water Res.* **2024**, *249*, No. 120941.
(23) Yan, P.-F.; Dong, S.; Woodcock, M. J.; Manz, K. E.; Garza-Rubalcava, U.; Abriola, L. M.; Pennell, K. D.; Cápiro, N. L. Biotransformation of 6:2 Fluorotelomer Sulfonate and Microbial Community Dynamics in Water-Saturated One-Dimensional Flow-through Columns. *Water Res.* **2024**, *252*, No. 121146.
(24) Weiner, B.; Yeung, L. W. Y.; Marchington, E. B.; D'Agostino, L. A.; Mabury, S. A. Organic Fluorine Content in Aqueous Film Forming Foams (AFFFs) and Biodegradation of the Foam Component 6:2 Fluorotelomermercaptoalkylamido Sulfonate (6:2 FTSAS). *Environ. Chem.* **2013**, *10* (6), 486−493.
(25) D'Agostino, L. A.; Mabury, S. A. Aerobic Biodegradation of 2 Fluorotelomer Sulfonamide−Based Aqueous Film−Forming Foam Components Produces Perfluoroalkyl Carboxylates. *Environ. Toxicol. Chem.* **2017**, *36* (8), 2012−2021.
(26) Li, R.; Munoz, G.; Liu, Y.; Sauvé, S.; Ghoshal, S.; Liu, J. Transformation of Novel Polyfluoroalkyl Substances (PFASs) as Co-Contaminants during Biopile Remediation of Petroleum Hydrocarbons. *Journal of Hazardous Materials* **2019**, *362*, 140−147.
(27) Liu, M.; Munoz, G.; Vo Duy, S.; Sauvé, S.; Liu, J. Stability of Nitrogen-Containing Polyfluoroalkyl Substances in Aerobic Soils. *Environ. Sci. Technol.* **2021**, acs.est.0c05811. 554698.
(28) Ruyle, B. J.; Schultes, L.; Akob, D. M.; Harris, C. R.; Lorah, M. M.; Vojta, S.; Becanova, J.; McCann, S.; Pickard, H. M.; Pearson, A.; Lohmann, R.; Vecitis, C. D.; Sunderland, E. M. Nitrifying Microorganisms Linked to Biotransformation of Perfluoroalkyl Sulfonamido Precursors from Legacy Aqueous Film-Forming Foams. *Environ. Sci. Technol.* **2023**, *57*, 5592.
(29) Dubocq, F.; Wang, T.; Yeung, L. W. Y.; Sjöberg, V.; Kärrman, A. Characterization of the Chemical Contents of Fluorinated and Fluorine-Free Firefighting Foams Using a Novel Workflow Combining Nontarget Screening and Total Fluorine Analysis. *Environ. Sci. Technol.* **2020**, *54* (1), 245−254.
(30) Cook, E. K.; Olivares, C. I.; Antell, E. H.; Yi, S.; Nickerson, A.; Choi, Y. J.; Higgins, C. P.; Sedlak, D. L.; Alvarez-Cohen, L. Biological and Chemical Transformation of the Six-Carbon Polyfluoroalkyl Substance N-Dimethyl Ammonio Propyl Perfluorohexane Sulfonamide (AmPr-FHxSA). *Environ. Sci. Technol.* **2022**, *56*, 15478.
(31) Wang, N.; Buck, R. C.; Szostek, B.; Sulecki, L. M.; Wolstenholme, B. W. 5:3 Polyfluorinated Acid Aerobic Biotransformation in Activated Sludge via Novel "One-Carbon Removal Pathways. *Chemosphere* **2012**, *87* (5), 527−534.
(32) *Perfluoroalkyl Substances in the Environment: Theory, Practice, and Innovation*; Kempisty, D. M.; Xing, Y.; Racz, L., Eds.; Environmental and Occupational Health Series; CRC Press/Taylor & Francis Group: Boca Raton, 2019.
(33) *ITRC (Interstate Technology & Regulatory Council). PFAS Technical and Regulatory Guidance Document and Fact Sheets PFAS-1*, 2023.
(34) Yan, P.-F.; Dong, S.; Manz, K. E.; Liu, C.; Woodcock, M. J.; Mezzari, M. P.; Abriola, L. M.; Pennell, K. D.; Cápiro, N. L. Biotransformation of 8:2 Fluorotelomer Alcohol in Soil from Aqueous Film-Forming Foams (AFFFs)-Impacted Sites under Nitrate-, Sulfate-, and Iron-Reducing Conditions. *Environ. Sci. Technol.* **2022**, *56* (19), 13728−13739.
(35) Dong, S.; Yan, P.-F.; Liu, C.; Manz, K. E.; Mezzari, M. P.; Abriola, L. M.; Pennell, K. D.; Cápiro, N. L. Assessing Aerobic Biotransformation of 8:2 Fluorotelomer Alcohol in Aqueous Film-Forming Foam (AFFF)-Impacted Soils: Pathways and Microbial Community Dynamics. *Journal of Hazardous Materials* **2023**, *446*, No. 130629.
(36) Dong, S.; Yan, P.-F.; Mezzari, M. P.; Abriola, L. M.; Pennell, K. D.; Cápiro, N. L. Using Network Analysis and Predictive Functional Analysis to Explore the Fluorotelomer Biotransformation Potential of Soil Microbial Communities. *Environ. Sci. Technol.* **2024**, *58* (17), 7480−7492.
(37) Löffler, F. E.; Sanford, R. A.; Ritalahti, K. M. Enrichment, Cultivation, and Detection of Reductively Dechlorinating Bacteria. In *Methods in Enzymology; Environmental Microbiology*; Academic Press, 2005; Vol. *397*, pp 77−111. .
(38) Bai, X.; Son, Y. Perfluoroalkyl Substances (PFAS) in Surface Water and Sediments from Two Urban Watersheds in Nevada, USA. *Science of The Total Environment* **2021**, *751*, No. 141622.
(39) Huang, S.; Sima, M.; Long, Y.; Messenger, C.; Jaffé, P. R. Anaerobic Degradation of Perfluorooctanoic Acid (PFOA) in Biosolids by Acidimicrobium Sp. Strain A6. *Journal of Hazardous Materials* **2022**, *424*, No. 127699.
(40) Li, F.; Fang, X.; Zhou, Z.; Liao, X.; Zou, J.; Yuan, B.; Sun, W. Adsorption of Perfluorinated Acids onto Soils: Kinetics, Isotherms, and Influences of Soil Properties. *Science of The Total Environment* **2019**, *649*, 504−514.
(41) Peter, K. T.; Phillips, A. L.; Knolhoff, A. M.; Gardinali, P. R.; Manzano, C. A.; Miller, K. E.; Pristner, M.; Sabourin, L.; Sumarah, M. W.; Warth, B.; Sobus, J. R. Nontargeted Analysis Study Reporting Tool: A Framework to Improve Research Transparency and Reproducibility. *Anal. Chem.* **2021**, *93* (41), 13870−13879.
(42) Williams, A. J.; Grulke, C. M.; Edwards, J.; McEachran, A. D.; Mansouri, K.; Baker, N. C.; Patlewicz, G.; Shah, I.; Wambaugh, J. F.; Judson, R. S.; Richard, A. M. The CompTox Chemistry Dashboard: A Community Data Resource for Environmental Chemistry. *J. Cheminform* **2017**, *9* (1), 61.
(43) Charbonnet, J. A.; McDonough, C. A.; Xiao, F.; Schwichtenberg, T.; Cao, D.; Kaserzon, S.; Thomas, K. V.; Dewapriya, P.; Place, B. J.; Schymanski, E. L.; Field, J. A.; Helbling, D. E.; Higgins, C. P. Communicating Confidence of Per- and Polyfluoroalkyl Substance Identification via High-Resolution Mass Spectrometry. *Environ. Sci. Technol. Lett.* **2022**, *9* (6), 473−481.
(44) Bugsel, B.; Zwiener, C. LC-MS Screening of Poly- and Perfluoroalkyl Substances in Contaminated Soil by Kendrick Mass Analysis. *Anal Bioanal Chem.* **2020**, *412* (20), 4797−4805.
(45) Maizel, A. C.; Shea, S.; Nickerson, A.; Schaefer, C.; Higgins, C. P. Release of Per- and Polyfluoroalkyl Substances from Aqueous Film-Forming Foam Impacted Soils. *Environ. Sci. Technol.* **2021**, *55*, 14617.
(46) Nickerson, A.; Maizel, A. C.; Kulkarni, P. R.; Adamson, D. T.; Kornuc, J. J.; Higgins, C. P. Enhanced Extraction of AFFF-Associated PFASs from Source Zone Soils. *Environ. Sci. Technol.* **2020**, *54* (8), 4952−4962.
(47) Choi, Y. J.; Helbling, D. E.; Liu, J.; Olivares, C. I.; Higgins, C. P. Microbial Biotransformation of Aqueous Film-Forming Foam Derived Polyfluoroalkyl Substances. *Science of The Total Environment* **2022**, *824*, No. 153711.
(48) Sörengård, M.; Franke, V.; Tröger, R.; Ahrens, L. Losses of Poly- and Perfluoroalkyl Substances to Syringe Filter Materials. *J. Chromatogr A* **2020**, *1609*, No. 460430.
(49) Favreau, P.; Poncioni-Rothlisberger, C.; Place, B. J.; Bouchex-Bellomie, H.; Weber, A.; Tremp, J.; Field, J. A.; Kohler, M. Multianalyte Profiling of Per- and Polyfluoroalkyl Substances (PFASs) in Liquid Commercial Products. *Chemosphere* **2017**, *171*, 491−501.
(50) Ochoa-Herrera, V.; Field, J. A.; Luna-Velasco, A.; Sierra-Alvarez, R. Microbial Toxicity and Biodegradability of Perfluorooctane Sulfonate (PFOS) and Shorter Chain Perfluoroalkyl and Polyfluoroalkyl Substances (PFASs). *Environ. Sci.: Processes Impacts* **2016**, *18* (9), 1236−1246.
(51) Rhoads, K. R.; Janssen, E. M.-L.; Luthy, R. G.; Criddle, C. S. Aerobic Biotransformation and Fate of *N* -Ethyl Perfluorooctane Sulfonamidoethanol (*N* -EtFOSE) in Activated Sludge. *Environ. Sci. Technol.* **2008**, *42* (8), 2873−2878.
(52) Yin, T.; Te, S. H.; Reinhard, M.; Yang, Y.; Chen, H.; He, Y.; Gin, K. Y.-H. Biotransformation of Sulfluramid (N-Ethyl Perfluorooctane Sulfonamide) and Dynamics of Associated Rhizospheric Microbial Community in Microcosms of Wetland Plants. *Chemosphere* **2018**, *211*, 379−389.

https://doi.org/10.1021/acs.est.4c08665
Environ. Sci. Technol. XXXX, XXX, XXX−XXX

(53) Zhang, L.; Lee, L. S.; Niu, J.; Liu, J. Kinetic Analysis of Aerobic Biotransformation Pathways of a Perfluorooctane Sulfonate (PFOS) Precursor in Distinctly Different Soils. *Environ. Pollut.* **2017**, *229*, 159−167.
(54) Liu, J.; Zhong, G.; Li, W.; Mejia Avendaño, S. Isomer-Specific Biotransformation of Perfluoroalkyl Sulfonamide Compounds in Aerobic Soil. *Science of The Total Environment* **2019**, *651*, 766−774.
(55) Chen, H.; Li, H.; Pei, S.; Wen, X.; Zhang, Y. Synthesis and Characterization of Fluoropoly(Amide−Sulfonamide)s via Polycondensation. *Polymer* **2009**, *50* (18), 4317−4324.
(56) Mejia Avendaño, S.; Liu, J. Production of PFOS from Aerobic Soil Biotransformation of Two Perfluoroalkyl Sulfonamide Derivatives. *Chemosphere* **2015**, *119*, 1084−1090.

https://doi.org/10.1021/acs.est.4c08665
Environ. Sci. Technol. XXXX, XXX, XXX−XXX